Oleate abrogates palmitate-induced lipotoxicity and pro-inflammatory response in human bone marrow-derived mesenchymal stem cells and osteoblastic cells

C. Gillet[1], D. Spruyt[1], S. Rigutto[1], A. Dalla Valle[1], J. Berlier[1], C. Louis[2], C. Debier[2], N. Gaspard[1], W.J. Malaisse[1], V. Gangji[1,3], J. Rasschaert[1]

[1]Laboratory of Bone and Metabolic Biochemistry, Faculty of Medicine, Université libre de Bruxelles, Brussels, Belgium; [2]Institute of Life Sciences (ISV), Université catholique de Louvain, Louvain-la-Neuve, Belgium; [3]Department of Rheumatology and Physical Medicine, Erasme Hospital, Brussels, Belgium

Osteoporosis is a metabolic bone disease associated with unequilibrated bone remodeling resulting from decreased bone formation and/or increased bone resorption, leading to progressive bone loss. In osteoporotic patients, low bone mass is associated with an increase of bone marrow fat resulting from accumulation of adipocytes within bone marrow (BM). BM adipocytes are active secretory cells, releasing cytokines, adipokines and free fatty acids (FA) that influence the BM microenvironment and altered the biology of neighboring cells. Therefore, we examined the influence of palmitate and oleate, two highly prevalent FA in human organism and diet, on the function and survival of human mesenchymal stem cells (MSC) and MSC-derived osteoblastic cells. The saturated FA palmitate exerted a cytotoxic action via initiation of endoplasmic reticulum stress and activation of the NF-κB and ERK pathways. In addition, palmitate induced a pro-inflammatory response, as determined by the upregulation of TLR4 expression as well as the increase of IL-6 and IL-8 expression and secretion. Moreover, we showed that MSC-derived osteoblastic cells were more sensitive to lipotoxicity than undifferentiated MSC. The monounsaturated FA oleate fully neutralized palmitate-induced lipotoxicity by impairing activation of the pathways triggered by the saturated FA. Moreover, oleate promoted palmitate detoxification by fostering its esterification into triglycerides and storage in lipid droplets.

Altogether, our data showed that physiological concentrations of palmitate and oleate differently modulated cell death and function in bone cells. We therefore propose that FA could influence skeletal health.

Osteoporosis is a metabolic bone disease prevalent in postmenopausal women and the elderly, associated with unequilibrated bone remodelling resulting from decreased bone formation and/or accelerated bone resorption. As a result, the refilling of resorption cavities can be incomplete, leading to progressive bone loss, increased bone fragility and fracture risk (1).

Bone formation is fulfilled by osteoblastic cells originating from the bone marrow-derived mesenchymal stem cells (MSC). MSC are pluripotent progenitor cells able to differentiate in osteoblastic cells and other cell types such as adipocytes and chondrocytes (2). Commitment of MSC to the osteoblast lineage is controlled by growth factors, hormones and cytokines and is sensitive to environmental conditions (3). In osteoporotic patients, the number of MSC is reduced and is correlated with an increased apoptosis of MSC and osteocytes (4). Moreover, osteoporosis is associated with adipocytes accumulation in the bone marrow niche due to a preferential differentiation of MSC toward adipocytes at the expense of osteoblast formation

ISSN Print 0013-7227 ISSN Online 1945-7170
Printed in USA

Received April 6, 2015. Accepted August 28, 2015.

Abbreviations:

(5, 6). Of note, a rise in bone marrow adiposity is also observed in ageing and, particularly, in secondary osteoporosis associated with glucocorticoids therapy or type 2 diabetes mellitus treatments such as PPARγ agonists (7–9).

Adipocytes are integral components of the bone marrow but their physiological function in the bone marrow stem cell niche and the consequence of their excessive accumulation in pathological entities remains elusive (10). Although they have long been considered as inert cells, it is now widely accepted that adipocytes constitute a metabolically active depot that may affect skeletal metabolism (11–14). By releasing factors such as fatty acids (FA), adipokines and cytokines, marrow adipocytes may generate a local microenvironment that could disturb bone cells viability and function (13, 15, 16). If the impact of cytokines and adipokines on bone health has been assessed, the effects of FA on the biological function and survival of MSC and osteoblastic cells have not yet been properly studied.

In physiological conditions, FA serve as key sources of cellular metabolic fuel and an acute exposure to these nutrients is usually beneficial for mammalian cells. Yet, a chronic exposure to FA may lead to ectopic lipid deposition in cells of nonadipose tissue. This unsuited FA accumulation is now increasingly recognized to contribute to organ injury through a process termed lipotoxicity (17). Sensitivity to lipotoxicity differs across cell types. In myocytes, hepatocytes and insulin-producing pancreatic beta cells, excessive FA availability results in cellular dysfunction and death (18–20), leading to disease states (17). If the contribution to lipotoxicity of long chain saturated and unsaturated FA varies depending on the cell type, FA toxicity is however often associated with the saturated ones (21).

We postulated that, in the setting of osteoporosis, excessive adipocytes accumulation in the bone marrow niche may favor the local release of larger quantities of saturated FA which could interfere with bone cells homeostasis. This hypothesis is supported by both in vitro and in vivo observations. Human primary coculture experiments of adipocytes originating from mammary adipose tissue and MSC-derived osteoblasts have shown that adipocytes liberate factors that inhibit preosteoblast proliferation and differentiation (22, 23). In a similar experimental model, MSC-derived adipocytes enhanced osteoblastic cells apoptosis via the release of saturated FA (24, 25). Recently, the study of Yeung et al demonstrated that the higher marrow fat content observed in osteoporotic subjects is characterized by an increased ratio of saturated vs unsaturated FA (26). Moreover, in diabetic patients, the proportion of saturated vs unsaturated FA in the marrow fat was associated with modifications of the fracture risk (27). Additionally, it is well known that diet FA profile (saturated, mono- or polyunsaturated) influences the FA profile of the triglycerides stored in adipocytes. Indeed, a higher consumption of saturated FA is negatively associated with bone mineral density (BMD) (28) and is linked to an increased risk of osteoporotic fractures (29).

The purpose of this study was therefore to examine the influence of FA on the function and survival of human MSC and osteoblastic cells. We selected two FA widely represented in human blood and diet (30): palmitate (Palm), a saturated FA (C16:0) and oleate (Ole), a monounsaturated one (C18:1 n-9). Palm and Ole have been extensively used in previous studies to evaluate the effects of FA on various cell types (31–33).

Our data showed that physiological concentrations of the two FA differently regulated cell death and function.

Materials and Methods

Isolation, culture and characterization of human MSC and MSC-derived osteoblastic cells

Human MSC were obtained from bone marrow aspirated from the posterior iliac crest of healthy donors (18–50 years old). Our local institutional ethical committee approved the study and all subjects gave their written consent. Bone marrow was diluted 1:0.5 with PBS and overlaid on Ficoll-Paque PREMIUM (GE Healthcare, Diegem, Belgium). Mononuclear cells were isolated after centrifugation and seeded at a density of 5.7×10^4 cells/cm^2 in DMEM low glucose (1 g/l; Invitrogen, Gent, Belgium) supplemented with 10% FBS (Sigma-Aldrich, Diegem, Belgium), 100 U/ml penicillin and 100 μg/ml streptomycin (Invitrogen). The culture medium was renewed after 4 days of culture and then every 2–3 days until cells reached confluence. MSC were detached by enzymatic treatment (Trypsin-EDTA; Invitrogen) every week and successively seeded at a density of 5.7×10^3 cells/cm^2 until passage 8.

To confirm the mesenchymal nature of the isolated cells, phenotyping by FACS flow cytometer and differentiation assays were performed. Cells were stained with the following antibodies: CD34-PE, CD45-FITC and CD73-PE from BD Biosciences (San Jose, USA), CD90-APC, CD105-FITC, and ALP-APC from R&D Systems (Abingdon, United Kingdom) (34). We confirmed that the cells expressed CD73, CD90, and CD105, and were negative for CD34, CD45 and ALP (Suppl. Figure 1A and B). Fluorescence was measured on a FACSCanto II flow cytometer (BD Biosciences) and data were processed using Diva software v5.0. At least 10 000 events were acquired for each sample. Supplemental validation showed that the cells had the capacity to differentiate in the osteoblastic and adipogenic lineage when cultured in standard in vitro differentiation assays (see below).

To obtain human MSC-derived osteoblastic cells (Ob), MSC were cultured for 14 days in an osteogenic medium (DMEM low glucose containing 10% FBS, 100 U/ml penicillin, 100 μg/ml streptomycin, 10 mM ß-glycerophosphate (Sigma-Aldrich), 10 nM dexamethasone (Sigma-Aldrich) and 50 μg/ml ascorbic acid

(Sigma-Aldrich). The culture medium was renewed every 2 days. The osteogenic medium was then replaced by standard culture medium for 48h. Osteoblastic differentiation was validated before FA treatment by mineralization assay (alizarin red staining) and measurement of alkaline phosphatase activity (ALP), as previously described (Suppl. Figure 1C) (35, 36). Induction of the osteoblastic differentiation marker genes Runt-related transcription factor 2 (Runx2) and Osteocalcin (OCN) was also confirmed by qPCR (Suppl. Figure 1D).

For adipogenic differentiation, MSC were cultured for 14 days in an adipogenic medium (DMEM low glucose containing 10% FBS, 100 U/ml penicillin, 100 μg/ml streptomycin, 60 μM indomethacin (Sigma-Aldrich), 0.5 mM 3-isobutyl-1-methylxanthine (Gibco), 5 μg/ml insulin (Sigma-Aldrich) and 100 nM dexamethasone (Sigma-Aldrich). The culture medium was renewed every 2 days. Adipogenesis was evaluated by Oil Red staining as previously described (Suppl. Figure 1C) (25).

SaOS-2 cells, a human osteoblastic cell line (a kind gift from Bone Therapeutics, Gosselies, Belgium) were grown in McCoy's 5A medium (Invitrogen) supplemented with 10% FBS, 100 U/ml penicillin and 100 μg/ml streptomycin.

Free fatty acid treatment

Sodium oleate and sodium palmitate (Sigma-Aldrich) were solubilized in 90% ethanol at 70°C to obtain 50 mM stock solutions. For FA supplementation experiments, cells were cultured for the indicated times in a FA-specific medium composed of DMEM low glucose (for MSC) or McCoy's 5A medium (for SaOS-2 cells) supplemented with 1% FBS, 100 U/ml penicillin, 100 μg/ml streptomycin, 1% FA free bovine serum albumin (BSA; Sigma-Aldrich) and, when required, diluted Palm and/or Ole (0.125 to 0.50 mM). Of note, a similar dilution of ethanol, the FA solvent, was added in the control condition (eg, absence of FA). Taking into account the stepwise equilibrium model and the respective binding affinities of Palm and Ole for BSA (37), the concentrations of FA used in our study are close to the physiological ones (30).

Determination of cell viability

Cells were seeded in 96-well plates at a density of 14.7×10^3 cells/cm^2 for MSC and Ob, and 20.6×10^3 cells/cm^2 for SaOS-2 cells. After 3 days, culture media were replaced by the FA-specific medium without or with increasing concentrations of Palm and/or Ole for the indicated times and concentrations. Cells were incubated for 15 minutes with the nuclear binding dyes propidium iodide (PI, 10 μg/ml, Sigma-Aldrich) and Hoechst 33 342 (HO 342, 10 μg/ml, Sigma-Aldrich). Cell viability was examined by inverted microscopy (Axiovision Zeiss, Zaventem, Belgium) with UV excitation (λ excitation/emission: 365/397 nm). Viable cells were characterized by their intact nuclei with blue fluorescence while dead cells were depicted by yellow-red fluorescence. In each experimental condition, a minimum of 600 cells were counted.

Measurement of caspases-3/7 activity

Caspases-3/7 activity was determined using the Caspase-Glo® 3/7 assay (Promega, Leiden, The Netherlands). 29.4×10^3 cells/cm^2 were seeded in 96-well white plates. After 3 days, culture media were replaced by FA-specific medium supplemented with increasing concentrations of Palm, complemented or not with Ole, for the indicated times. At the end of the incubation period, 100 μl of culture medium were replaced by 100 μl of Caspase-Glo reagent resulting in cell lysis and cleavage of the Caspase-Glo® 3/7 substrate by the activated caspases. The luminescent signal generated was detected after 1 hour using a Victor2 (PerkinElmer, Zaventem, Belgium). Staurosporin 1 μM (Sigma-Aldrich) was used as positive control.

Measurement of NF-κB activation

SaOS-2 cells were plated in 8-chamber slides (BD Biosciences) at a density of 14.5×10^3 cells/cm^2. After 3 days, culture media were replaced by FA-specific medium supplemented with Palm and/or Ole, for the indicated times. Cells treated for 1 hour with 30 UI/ml recombinant human (rh) IL-1β (R&D systems) were used as positive control. To evaluate NF-κB nuclear translocation by immunocytochemistry, cells were fixed with 4% formaldehyde for 10 minutes, and permeabilized with an acetone/methanol (7:3) mixture for 5 minutes. Nonspecific binding sites were blocked with 10% normal goat serum (Gibco, Gent, Belgium) and 0.8% BSA fraction V (Sigma-Aldrich) for 30 minutes. Cells were then incubated overnight with rabbit polyclonal antibody raised against NF-κB p65 (1:500, Santa Cruz Biotechnology, Heidelberg, Germany). Finally, cells were incubated for 1 hour with donkey antirabbit IgG-fluorescein isothiocyanate (FITC), (1:200, Jackson IR, Newmarket, United Kingdom) and nuclei were stained with HO 342. Cells were mounted using the Dako fluorescence mounting medium (Dako, Heverlee, Belgium) and examined with inverted fluorescence microscope (Axio Zeiss).

Our results were confirmed in SaOS-2 and MSC extract samples, using a NF-κB p65 ELISA kit following the manufacturer's instructions (Fisher Scientific, Aalst, Belgium).

Quantification of mRNA expression by quantitative polymerase chain reaction (PCR) (qPCR)

Total RNA was isolated from MSC, Ob cells and SaOS-2 cells seeded for 3 days before treatment in 6-well plates at a density of 10.4×10^3 cells/cm^2, using AURUM^{TM} kit (Bio-Rad, Nazareth Eke, Belgium) according to the manufacturer's protocol. Total

Table 1. Antibody Table

Peptide/protein target	Antigen sequence (if known)	Name of Antibody	Manufacturer, catalog #, and/or name of individual providing the antibody	Species raised in; monoclonal or polyclonal	Dilution used
Phospho-p44/42 MAPK (Erk1/2)	(Thr202/Tyr204)	Phospho-p44/42 MAPK (Erk1/2) (Thr202/Tyr204) Antibody	Cell Signaling, #9101	Polyclonal	1/1000
p44/42 MAPK (Erk1/2)	/	Anti-MAP Kinase 1/2 (Erk1/2), CT	MILLIPORE, #06–182	Polyclonal	1/1000
Phospho-eIF2α	(Ser51)	Phospho-eIF2α (Ser51) (D9G8) XPTM Rabbit mAB	Cell Signaling, #3398	Monoclonal	1/1000
eIF2α	/	eIF2α (D7D3) XPTM Rabbit mab	Cell Signaling, #5324	Monoclonal	1/1000
NF-κB	/	NF-κB p65 (C-20)	Santa Cruz, sc-372	Polyclonal	1/500

RNA was reverse transcribed using iScriptcDNA synthesis kit (Bio-Rad).

qPCR reactions were performed using a CFX96 thermal system (Bio-Rad) in a total reaction volume of 20 μl containing 3 mM $MgCl_2$, 0.3 μM (each) forward and reverse primers (Eurogentec, Seraing, Belgium), 10 μl SYBR Green mix (Bio-Rad), and 2 μl cDNA (10 ng/μl). The cycling program was as follow: 95°C for 3 minutes followed by 40 cycles at 95°C for 30 seconds and 60°C for 30 seconds. All reactions were performed in duplicate. Expression of Toll-like receptor-4 (TLR4) was quantified by qPCR using the standard curve method (38) and the appropriate primer sets (Supplementary material, Table 1). Relative mRNA expression of the other target genes was evaluated using the comparative threshold cycle method ($2^{-\Delta\Delta Ct}$) and adequate primer sets (Supplementary material, Table 2). Hypoxanthine phosphoribosyltransferase 1 (HPRT1) was used as housekeeping gene.

To study X-box binding protein 1 (XBP1) splicing, cDNA were amplified by standard PCR (cycling program: 94°C for 45 seconds, 58°C for 20 seconds and 72°C for 1 minute; 24 cycles) using XBP1 specific primers (Supplementary material, Table 1). XBP1 expression was normalized for HPRT1 expression. Ten μl of the PCR reaction mixture were analyzed on a 2% agarose gel and bands were visualized using Fusion UV System equipment (Vilber Lourmat, Marne-La-Vallée, France).

Western blotting

Human MSC treated with FA were lyzed with Laemmli buffer (10% glycerol, 0.5 mM DTT, 63 mM Tris-HCl, 1% SDS, pH 6.8) containing a cocktail of proteases and phosphatases inhibitors (Roche Diagnostics, Vilvoorde, Belgium). Proteins were quantified by a paper dye binding assay. Equal protein amounts were separated by SDS-PAGE using 10% or 12% polyacrylamide gels. Proteins were transferred on polyvinylidene difluoride (PVDF) membranes Immobilion-P (Millipore, Overijse, Belgium) and immunolabeled overnight at 4°C using the following antibodies: anti-phospho-eIF2α^{Ser51} and anti-phospho-ERK-$^{Thr202/Tyr204}$ (Cell Signaling Technology, Bioké, Leiden, The Netherlands). The secondary antibodies peroxidase-conjugated ECL™ (GE healthcare) were used for 1 hour at room temperature. The immune complexes were detected by using the enhanced chemiluminescence method (Western Lightning® *Plus*-ECL, PerkinElmer Inc, Zaventem, Belgium). Band densities were quantified by ImageJ program (NIH, Bethesda, USA). Results were expressed as relative ratio between the phospho- and the total proteins, which were detected with the following antibodies: anti-eIF2α (Cell Signaling Technology) or anti-ERK (Millipore).

Measurement of IL-6 and IL-8 production

Supernatants of MSC were collected after 48 hours of treatment with FA, aliquoted and frozen at –20°C until use. IL-6 and IL-8 concentrations were measured by ELISA according to the manufacturer's protocol (Duoset™, R&D systems).

Detection of intracellular lipid droplets (LD) and characterization of their neutral lipids content

After 16 hours incubation with FA, SaOS-2 cells were washed twice with PBS and fixed with 4% paraformaldehyde for 15 minutes. Neutral lipids accumulated in intracellular LD were stained with Oil Red O (Sigma-Aldrich) for 2 hours and rinsed twice with PBS before microscopic observation. To evaluate the cellular content of neutral lipids, cells were washed with PBS, scrapped and collected in 1 ml lysis buffer (1% SDS, 60 mM Tris-HCl and 10 mM EDTA). Total lipids were extracted with chloroform/methanol/water (2:2:1). Isolation of cellular neutral lipids and analysis of their FA content were performed according to Louis et al 2014 (39).

Statistical analysis

Data are presented as means ± SEM. Values were determined from at least three independent experiments. Statistical analysis was performed using Student's *t* test or one-way ANOVA followed by *t* test with the Bonferroni correction for multiple comparisons. Differences between groups were considered as statistically significant at $P < .05$.

Results

Oleate prevents palmitate-induced lipotoxicity

To evaluate the sensitivity of human MSC and Ob to lipotoxicity, cells were exposed to increasing concentrations of Palm (0.125 to 0.50 mM) and/or Ole (0.25 mM) for 24 to 72 hours. Palm elicited cell mortality in a time- and dose-dependent manner in both cell types and our data demonstrated that Ob were more sensitive to lipotoxicity than MSC. Indeed, as showed in Figure 1A and B, a treatment for 48 hours with 0.50 mM of the saturated FA reduced cell viability to 50 ± 3.9% in MSC ($P < .001$ vs Ctrl) and to 11.8 ± 3.4% in Ob ($P < .001$ vs Ctrl). Similar observations were obtained in SaOS-2 cells (Suppl. Figure 2A). By contrast, Ole did not affect cell viability (data not shown) but, rather, completely prevented the harmful effect of Palm (Figure 1A and B). The cytoprotective action of Ole was maintained even when the culture period was extended to 7 days and when the concentration of Ole was decreased to 0.05 mM (data not shown).

To determine whether cell death was associated with apoptosis, caspases-3/7 activity was evaluated after 24 hours and 48 hours of treatments. Palm toxicity coincided with a dose- and time-dependent increase of caspases-3/7 activity in MSC (Figure 1C). The beneficial effect of Ole on Palm cytotoxicity was reflected by a complete suppression of caspases activation, which persisted even when Ole was tested at 0.05 mM (Figure 1C). Similar results were obtained in SaOS-2 cells (Suppl. Figure 2B) and Ob (Suppl. Figure 2C).

Oleate abolishes palmitate-induced ERK and NF-κB activation

ERK and NF-κB pathways control cell survival. We therefore evaluated the effects of Palm and Ole on ERK activation. Our results showed that Palm stimulated ERK

phosphorylation in MSC which was suppressed by addition of Ole (Figure 2A). Similar results were obtained with SaOS-2 cells (Suppl. Figure 3).

In parallel, we evaluated the effect of Palm on activation of NF-κB, a transcription factor ensuring a proapoptotic role in Ob (40). As illustrated in Figure 2B, Palm stimulated NF-κB nuclear translocation in SaOS-2 cells, which did not occur when Palm was associated with Ole. Similar results were obtained in MSC by ELISA (Suppl. Figure 4).

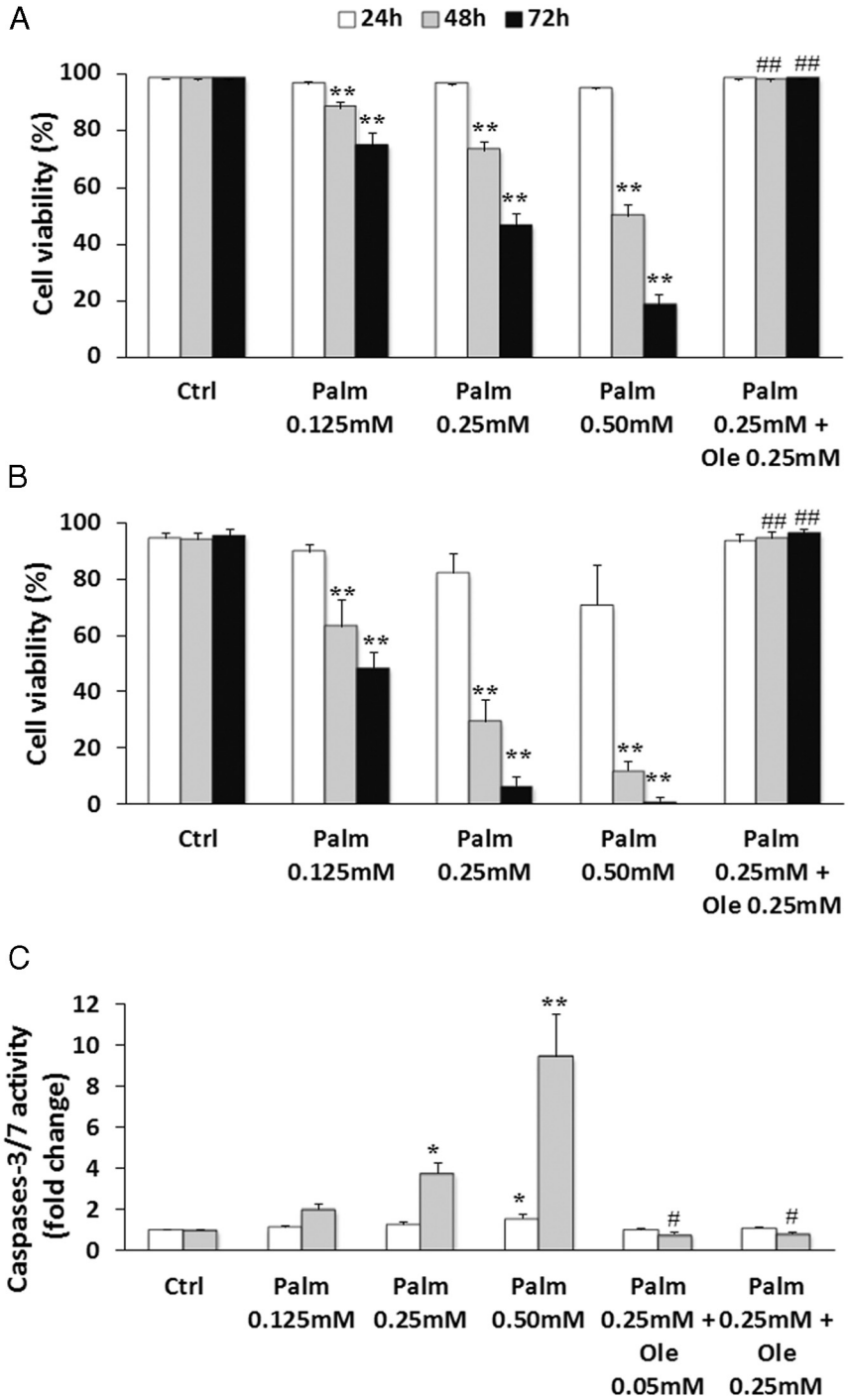

Figure 1. Oleate suppressed palmitate-induced cytotoxicity in MSC and Ob. MSC (A,C) and Ob (B) were treated with increasing concentrations of Palm (0.125 mM to 0.50 mM) ± Ole (0.05 mM or 0.25 mM) for the indicated times. (A,B) Cell viability was quantified by nuclear staining with Hoechst and propidium iodide. Values are mean ± SEM of 15 (MSC) or 5 (Ob) individual experiments. $^{**}P < .001$ vs appropriate control condition (Ctrl, 24, 48 or 72 hours); $\#\#P < .001$ vs 0.25 mM Palm. C, Caspases-3/7 activity was measured using the Caspases-3/7 Glo assay. Values are expressed relative to Ctrl and are mean ± SEM of 7 individual experiments. $^{*}P < .01$, $^{**}P < .001$ vs appropriate control (Ctrl, 24 or 48 hours); $\#P < .01$ vs 0.25 mM Palm.

Oleate blocks palmitate-induced proinflammatory response

In immune cells, the activation of NF-κB and ERK pathways induces an inflammation process through the transcriptional regulation of cytokines and chemokines. MSC are known to secrete soluble factors in response to stress conditions such as hypoxia or hyperglycemia (41, 42). However, little information is available concerning the effects of Palm and Ole on cytokines regulation in MSC and Ob. Our results showed that, after 24 hours of treatment, Palm triggered IL-6 (Figure 3A) and IL-8 (Figure 3B) expression in MSC and Ob, while it did not affect chemokine (C-C motif) ligand 2 (CCL2, MCP1) expression (data not shown). Of note, Palm-induced cytokines expression was higher in Ob than in MSC (Figure 3A & B). Coincubation of the saturated FA with Ole prevented IL-6 and IL-8 gene upregulation in both cell types (Figure 3A &B). In parallel, we assessed IL-6 and IL-8 secretion in MSC. Palm triggered the secretion of both cytokines, which was abrogated by Ole (Figure 3C), as observed for gene expression.

TLRs detect exogenous pathogen-associated molecular patterns and initiate cytokines and chemokines secretion via ERK and NF-κB pathways activation. Interestingly, TLR4 is also able to trigger immune responses after the detection of endogenous ligands such as the long chain FA Palm and stearate (43). We observed that, after 24 hours of treatment, Palm increased dose-dependently TLR4 expression in MSC

and, to a more marked extent, in Ob (Fig. 4). Ole alone did not alter TLR4 expression (data not shown) but repressed Palm-induced gene up-regulation (Fig. 4). Similar data were obtained in SaOS-2 cells (data not shown). Therefore, to examine the contribution of TLR4 in Palm-induced lipotoxicity, we used MSC isolated from Warthon jelly (WJ-MSC) as they do not express TLR4 (44). We observed that WJ-MSC were as susceptible to lipotoxicity as MSC isolated from bone marrow (Suppl. Figure 5).

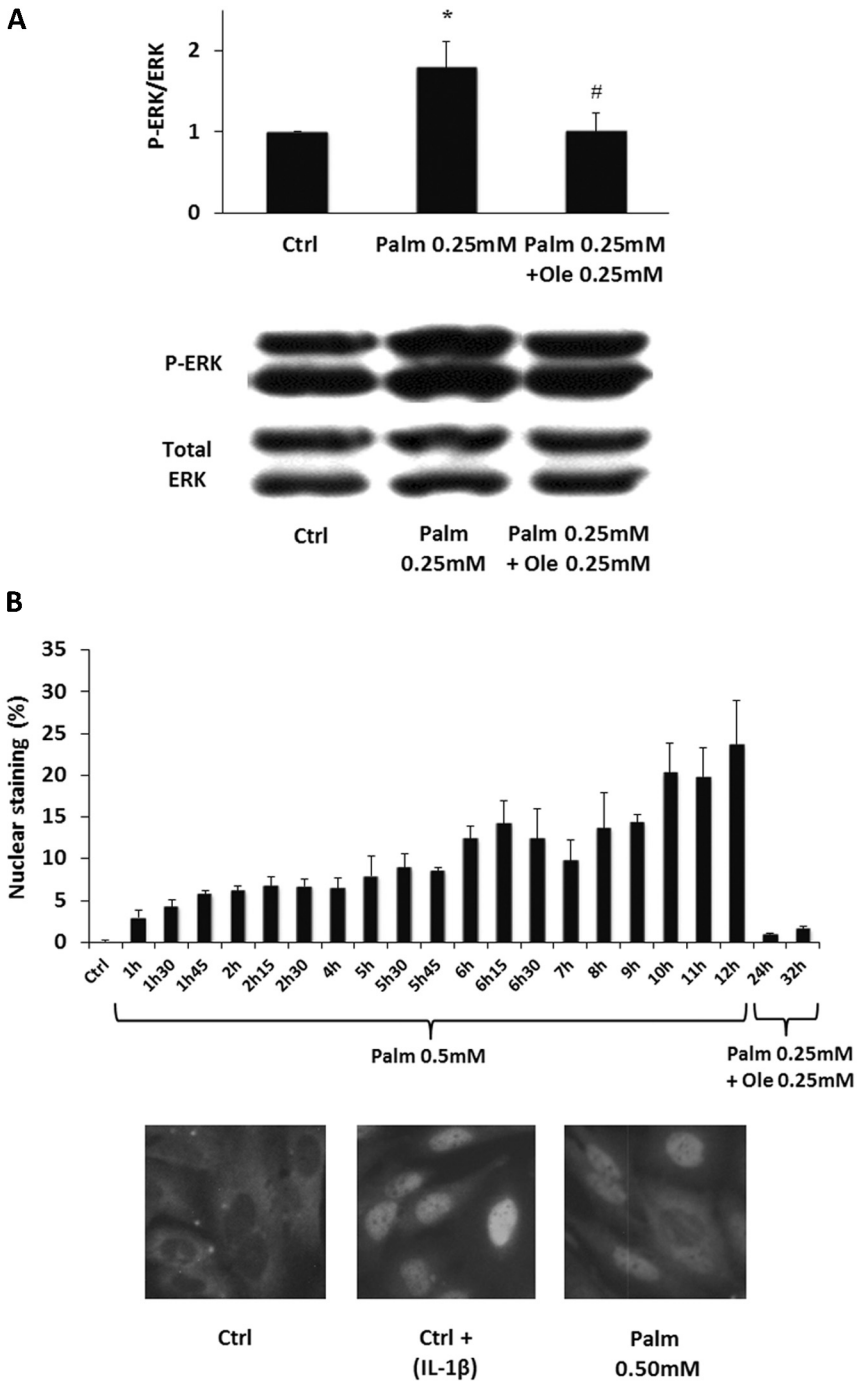

Figure 2. Oleate blocked palmitate-induced activation of ERK and NF-κB. A, MSC were treated for 48 hours with 0.25 mM Palm ± 0.25 mM Ole. ERK phosphorylation was evaluated by Western blotting and normalized for total ERK. The western blot is representative of 1 out of 4 individual experiments. Values are mean ± SEM. *$P < .05$ vs Ctrl, #$P < .05$ vs 0.25 mM Palm. B, SaOS-2 cells were treated with 0.50 mM Palm or 0.25 mM Palm plus 0.25 mM Ole. Nuclear translocation of NF-κB was regularly evaluated by immunocytochemistry. Values presented as the percentage of stained nuclei are means ± SEM of 6 individual experiments. Representative immunocytochemistry results of NF-κB nuclear translocation. IL-1β was used as positive control.

Oleate abrogates palmitate-induced endoplasmic reticulum (ER) stress activation

ER stress was recently implicated in Palm-induced apoptosis in human MSC (45). Therefore, we evaluated whether the protective action of Ole could be mediated through prevention of ER stress initiation in MSC and Ob by different approaches. First, we measured the expression levels of well-known ER stress marker genes such as the transcription factors C/EBP homologous protein (CHOP), activating transcription factor 4 (ATF4) and XBP1. A 24 hours treatment with Palm up-regulated the expression of the selected genes in both MSC and Ob (Figure 5A-C). Interestingly, the impact of the saturated FA on gene expression was more marked in Ob than in MSC. Moreover, Palm activated the cleavage of XBP1 mRNA (Fig. 5D). Ole abolished Palm-induced gene up-regulation and XBP1 splicing in both cell types (Figure 5).

Secondly, we evaluated the activation of the unfolded protein response (UPR), a signaling network initiated in response to severe ER stress. The shut-down of protein synthesis was assessed by measuring the phosphorylation of the alpha subunit of the eukaryotic initiation factor 2 (eIF2) and the expression of the Ca^{2+}-sensitive chaperone binding immunoglobulin protein (BiP) was determined by qPCR. Our results demonstrated that Palm treatment led to overexpression of BiP (Figure 6A) and increased eIF2α phosphorylation in MSC (Fig. 6B-C). Addition of Ole suppressed BiP expression (Fig. 6A) and restored eIF2α phos-

phorylation to its control levels (Fig. 6B-C). Similar results were obtained in SaOS-2 cells (data not shown).

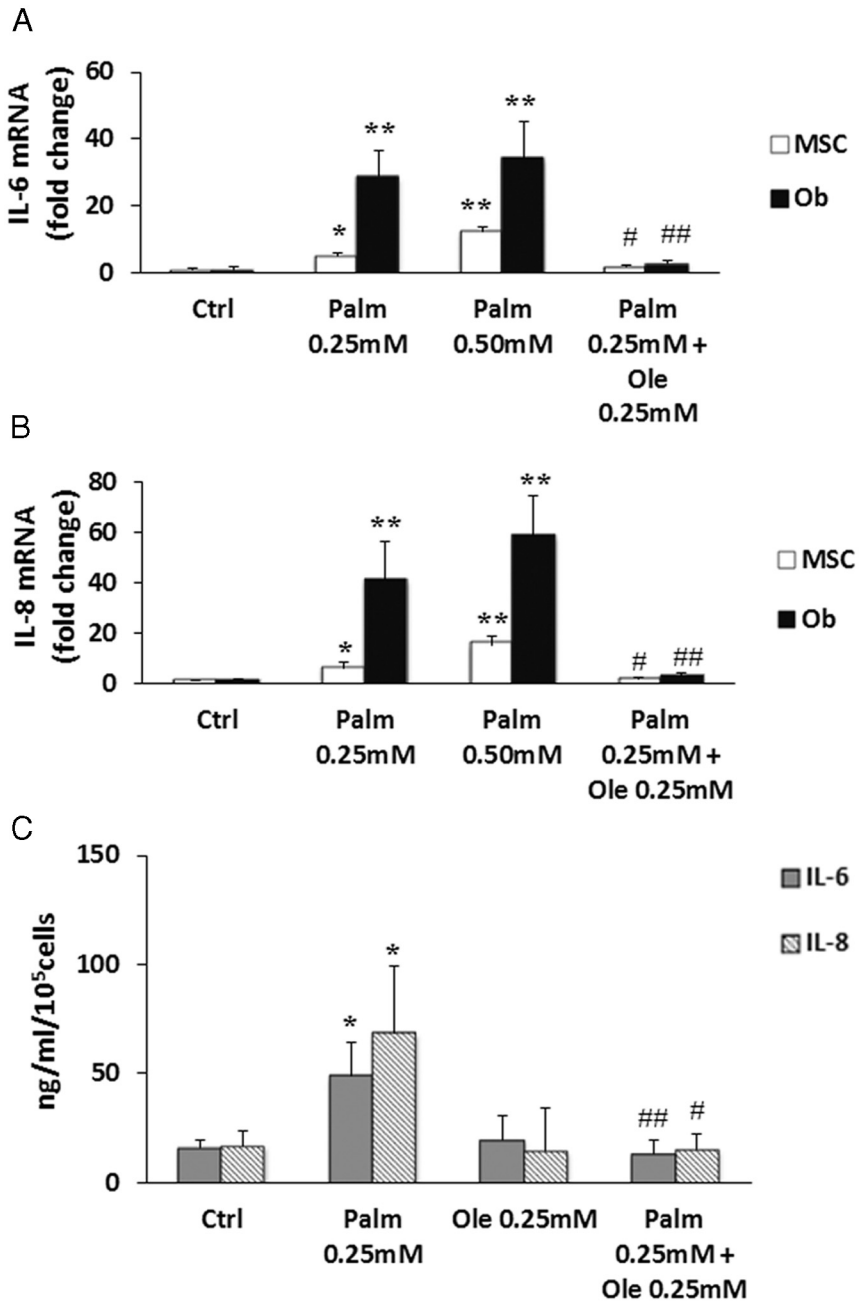

Figure 3. Oleate prevented IL-6 and IL-8 expression stimulated by palmitate. MSC and Ob were treated for 24h with increasing concentrations of Palm (0.25 mM to 0.50 mM) ± 0.25 mM Ole. IL-6 (A) and IL-8 (B) expression were quantified by qPCR using the ΔΔCT method compared to Ctrl. Values were normalized for HPRT1 expression and are represented as means ± SEM of 6 individual experiments. *$P < .01$, **$P < .001$ vs Ctrl, #$P < .01$, ##$P < .001$ vs 0.25 mM Palm. C, IL-6 and IL-8 secretions were quantified in supernatants of MSC treated 48 hours with 0.25 mM Palm ± 0.25 mM Ole using ELISA kit. Values were normalized for 100 000 cells and are represented as means ± SEM of 7 individual experiments. *$P < .05$ vs Ctrl, #$P < .05$, ##$P < .01$ vs 0.25 mM Palm.

Oleate, but not palmitate, induces lipid droplets formation

In situations of excessive FA exposure, triglycerides (TG) may accumulate in intracellular LD that have now gain recognition as dynamic organelles involved in various cellular processes (46). We therefore evaluated the capacity of Palm and Ole to induce LD formation in osteoblastic cells. As illustrated in Figure 7A, after 16 hours of treatment, SaOS-2 cells cultured in control conditions or in the presence of Palm did not present LD. However, Ole, tested alone or in the concomitant presence of Palm, triggered LD formation (Figure 7A). We further quantified and characterized the neutral lipids content (mainly composed of mono-, di-, and TG) of SaOS-2 cells exposed to Palm and/or Ole (Figure 7B). In the absence of FA, the cellular neutral lipids content amounted to 3.4 ± 1.4 $\mu g/10^6$ cells. Increased concentrations of Palm (0.125 mM to 0.50 mM) tended to augment ($P = .08$) the cellular neutral lipids content whereas 0.25 mM Ole was sufficient to induce a 7.3-fold increase ($P = .018$) of total neutral lipids (Figure 7B). When compared to 0.25 mM Ole alone, the concomitant presence of Palm and Ole (0.25 mM each) did not modify the total lipid content. Nevertheless, when compared to 0.25 mM Palm, the addition of Ole increased by 3.4 fold the incorporation of Palm into the neutral lipids fraction ($P < .001$; Figure 7B).

Discussion

Fat is an integral component of the bone marrow microenvironment but its physiological function and its role in the pathogenesis of metabolic bone diseases are still under debate. In osteoporotic patients and in the context of ageing, an inverse relation between marrow adipose tissue (MAT) and bone mass is now well established (47, 48). However, in an-

imal models, obesity or a high fat diet may trigger various bone responses ranging from preserved bone density (49) to decreased bone mass and quality (50–52). In humans, obesity was previously often correlated with a higher bone mass density (53, 54) but it may also adversely alter bone quality and contribute to an increased fracture risk (55, 56). Recent studies demonstrate that bone mass and MAT are inversely correlated in healthy subjects (57, 58). On the whole, these data demonstrate the complexity of the relationship between exogenous lipid intake, MAT and bone health. Of note, the concept that the FA profile as well as the amount of marrow adipocytes may be relevant for skeletal preservation is emerging (59, 60).

Recent experimental data suggest that FA and lipotoxicity could play a role in the initiation and/or evolution of metabolic bone diseases such as osteoporosis.

In the present study we evaluated the effect of Palm and Ole, the most common saturated and monounsaturated FA found in human serum and in the Western diet (30). Of note, Palm was recently identified as one of the FA predominantly liberated in the culture medium by MSC-derived adipocytes (25). The effect of Palm and Ole were extensively studied in cell types implicated in disorders of energy metabolism (ie, hepatocytes, insulin-producing pancreatic beta cells, myocytes). However, the concept of lipotoxicity recently emerged in skeletal cells and the few studies conducted on human bone marrow-derived MSC and MSC-derived osteoblastic cells focused on the action of Palm (25, 31, 35, 36, 45). The studies addressing the effect of Ole are rare and diverging. While the recent work of Fillmore et al (61) demonstrated that Ole abrogated Palm-induced impairment of MSC metabolism, two previous studies indicated that Ole is toxic for MSC, does not prevent Palm-induced toxicity and increases Palm-triggered apoptosis (31, 62).

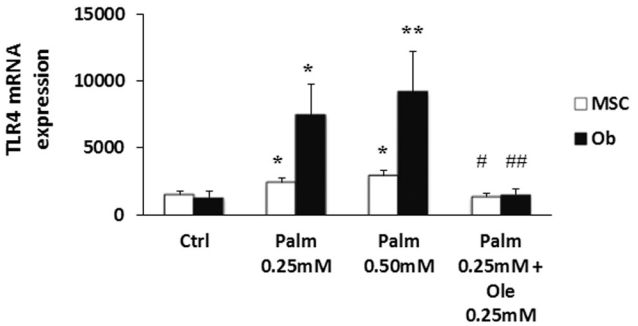

Figure 4. Oleate abolished palmitate–induced expression of TLR4. MSC and Ob were treated for 24 hours with Palm (0.25 mM to 0.50 mM) ± 0.25 mM Ole. TLR4 expression was quantified by qPCR using standard curve method and normalized for HPRT1.Values are mean ± SEM of 6 individual experiments. *$P < .05$, **$P < .01$ vs Ctrl; #$P < .05$, ##$P < .01$ vs Palm 0.25 mM.

We demonstrated that Palm and Ole inversely regulate cell death and function of human MSC and osteoblastic cells. We confirmed that Palm elicits cell death and showed

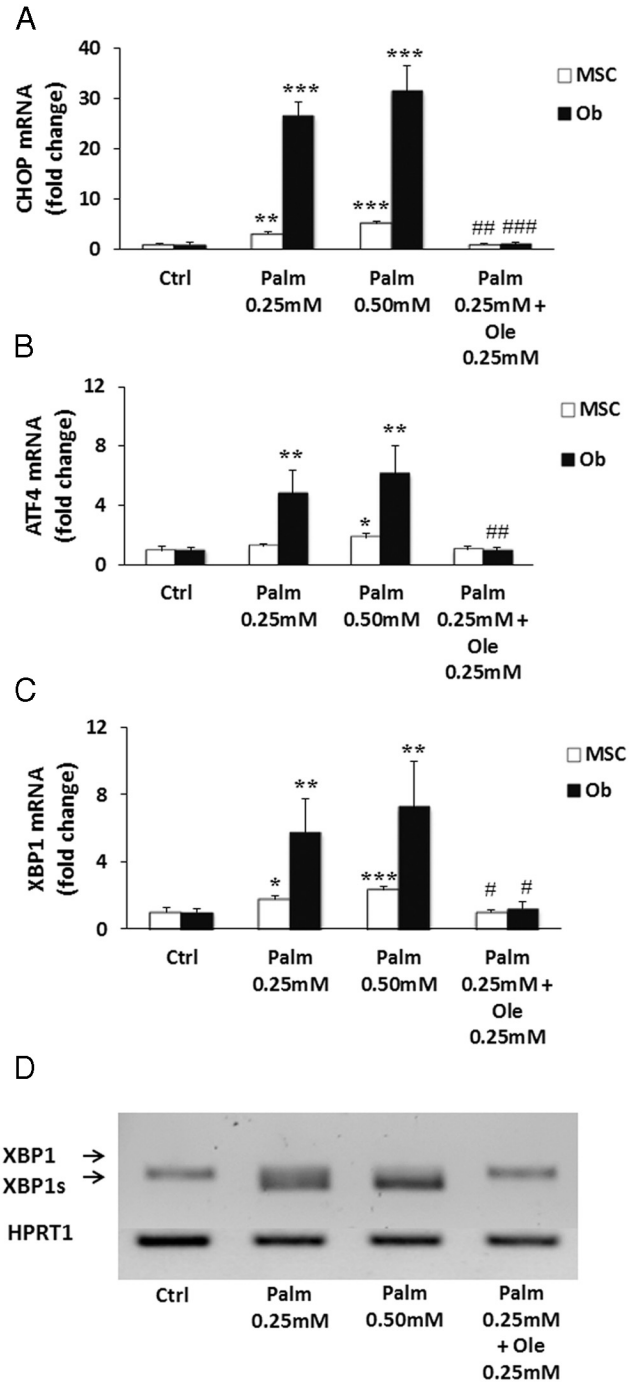

Figure 5. Oleate blocked ER stress markers expression and activation of palmitate-induced XBP splicing. MSC and Ob were treated for 24h with 0.25 mM Palm ± 0.25 mM Ole. CHOP (A), ATF4 (B) and XBP1 (C) expression were quantified by qPCR using the ΔΔCT method. Values were normalized for HPRT1 expression and are expressed as the ΔΔCT compared to Ctrl. Results are means ± SEM of 6 individual experiments. * $P < .05$, ** $P < .01$, *** $P < .001$ vs Ctrl; # $P < .05$, ## $P < .01$, ### $P < .001$ vs Palm 0.25 mM. D, Representative PCR results for XBP1 splicing, compared to HPRT1 expression, of 1 out of 6 individual experiments in MSC.

that Ob are more sensitive to lipotoxicity than MSC. We established that the monounsaturated FA Ole is not toxic for MSC and osteoblastic cells but that it completely abrogates Palm-induced lipotoxicity and proinflammatory response.

Depending on the cell type, lipotoxicity is related to the initiation of different cellular mechanisms (21). We thus further clarified the molecular mechanisms underlying the cytotoxic and cytoprotective actions of the two FA in MSC and osteoblastic cells since their understanding may pave the way for innovative therapeutic approaches.

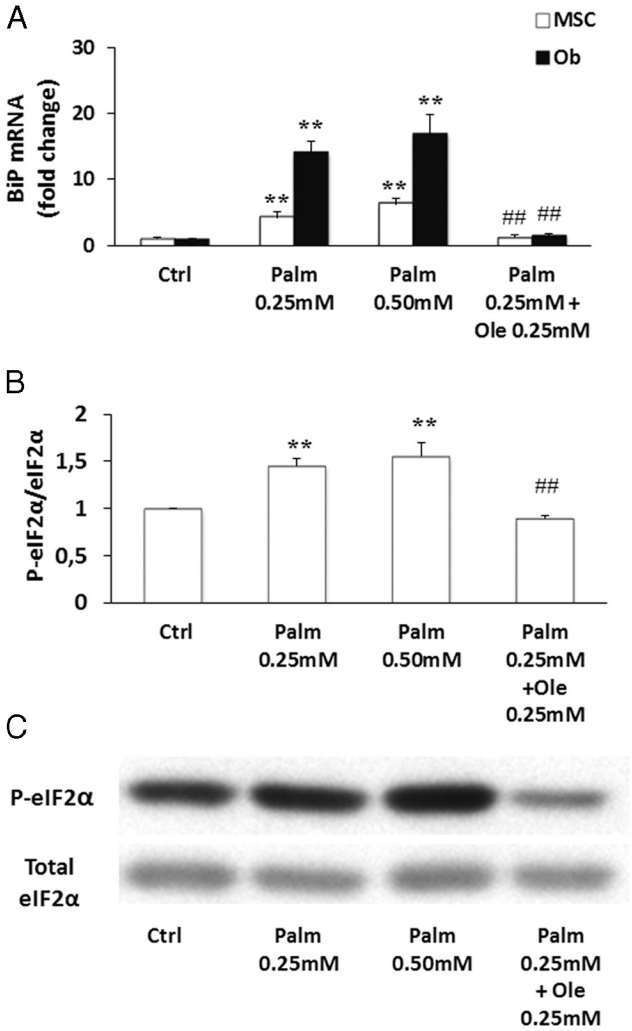

Figure 6. Oleate prevented palmitate-triggered eIF2α activation and BiP expression. MSC were treated for 24 and 48 hours with increasing concentrations of Palm (0.25 mM to 0.50 mM) ± Ole 0.25 mM. A, BiP expression was quantified by qPCR using the ΔΔCT. Values were normalized for HPRT1 expression and are expressed as the ΔΔCT compared to the control (Ctrl). Results are mean ± SEM of 6 individual experiments. B, Expression of phosphorylated eIF2α was evaluated by Western blotting and normalized for total eIF2α. Values are mean ± SEM. $^{**}P < .001$ vs Ctrl, $^{\#\#}P < .001$ vs Palm 0.25 mM. C, The Western blotting figure is representative of 1 out of 4 individual experiments.

ERK activation may lead to cell death or survival. A recent study showed that Palm activates ERK phosphorylation in MSC (45), while contradictory data were obtained in osteoblastic cells (31, 35). We showed that Palm triggers ERK phosphorylation in MSC and osteoblastic cells; Ole does not affect ERK pathway but prevents its activation by Palm. Furthermore, we demonstrated that Palm activates the transcription factor NF-κB, a phenomenon counteracted by Ole. NF-κB plays a proapoptotic role in osteoblastic cells and its activation was associated with lipotoxicity-induced ER stress in other cell types (40, 63). Thus, Ole could protect MSC and Ob from Palm-induced lipotoxicity by preventing the initiation of two proapoptotic pathways.

In MSC, ERK and NF-κB pathways regulate cytokines and chemokines secretion and can be activated following TLRs stimulation by exogenous ligands. The effects of FA on cytokines production and TLRs expression have not yet been investigated in human MSC and osteoblastic cells. We showed that Palm triggers TLR4, IL-6 and IL-8 expression and secretion that were completely suppressed by Ole. Palm-induced cytokines and TLR4 expression was higher in Ob than in MSC. Chronic inflammation is associated with aging and induces bone loss and osteoporosis (64). Interestingly, a growing number of studies related to metabolic diseases points to a link between enhanced circulating FA levels and the induction of a chronic inflammatory process via TLRs stimulation (65). TLRs perpetuate inflammatory responses through the recognition of exogenous pathogen-associated molecular patterns and endogenous ligands. For example, TLR4 is able to trigger immune responses after the detection of long chain FA (43). MSC constitutively express the proinflammatory cytokines IL-6 and IL-8. However, the overproduction of these cytokines stimulates the differentiation of osteoclast precursor cells to mature osteoclasts (66, 67). By enhancing IL-6 and IL-8 production, Palm could thus promote a proinflammatory state favoring bone resorption and impairing bone formation. In line with this hypothesis, IL-6 and IL-8 levels are increased in both the synovial fluid and the serum of patients suffering from chronic inflammatory diseases predisposing to osteoporosis (68, 69).

To clarify the role of TLR4 in Palm-induced lipotoxicity, we used WJ-MSC that do not express TLR4 (44). WJ-MSC were as susceptible to Palm as MSC isolated from bone marrow, suggesting that TLR4 does not mediate lipotoxicity in MSC and osteoblastic cells. However, TLR2 may also recognize FA (43). TLR2 is expressed in WJ-MSC (44) and we observed that it is upregulated by Palm (data not shown). Therefore, the functional role of

TLR4 and/or TLR2 in Palm-induced lipotoxicity should not be excluded and requires further investigations.

Saturated FA are major ER-stress inducers in pancreatic beta cells (70) and it has recently been shown that FA-induced MSC apoptosis implicate ER stress activation (45). Altogether, our results showed that Palm triggered ER stress and UPR in both MSC and osteoblastic cells. The ER stress response is more severe in Ob, which correlates

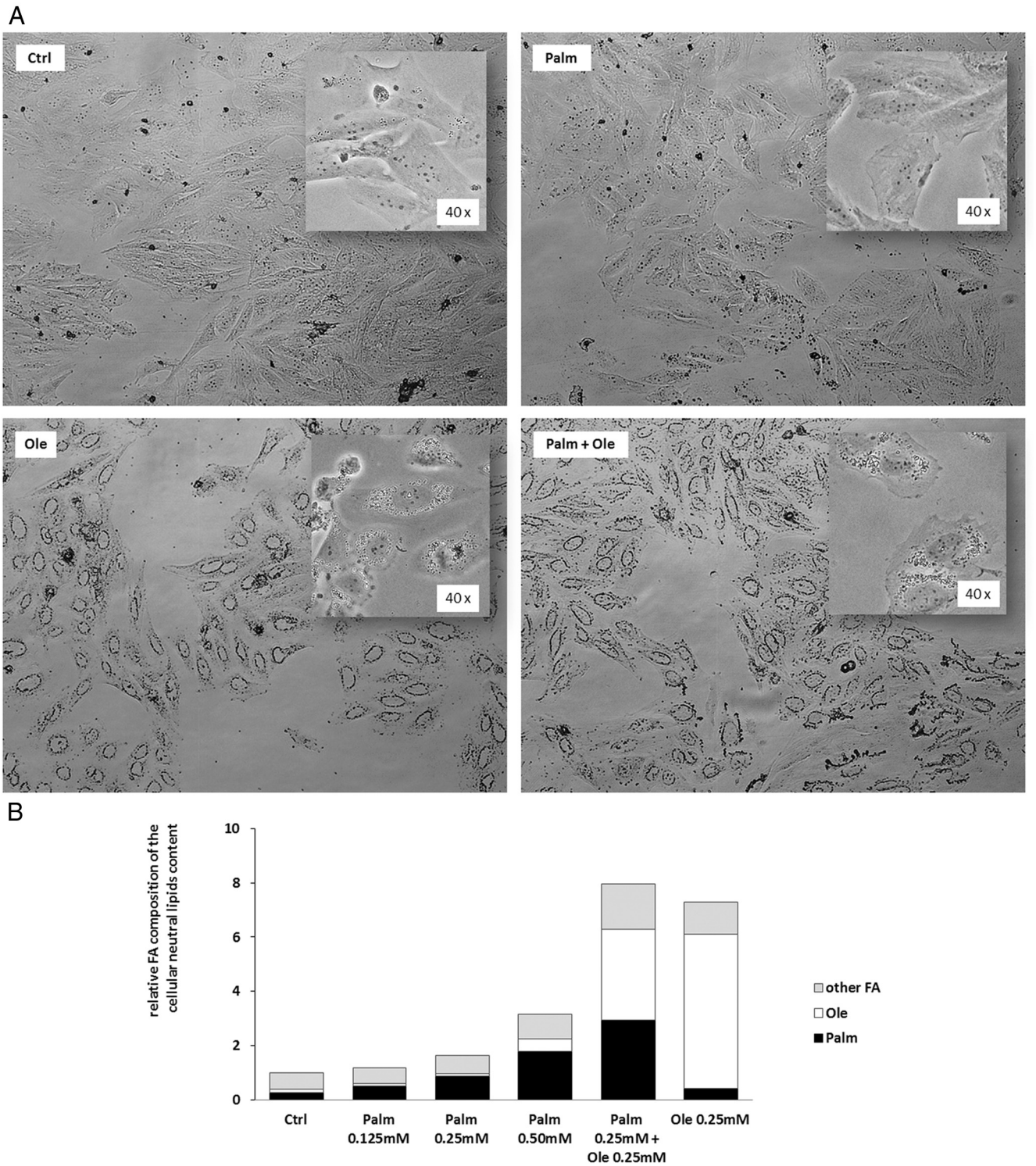

Figure 7. Oleate but not palmitate, enhanced lipid droplets formation and promoted palmitate incorporation into the neutral lipids fraction. SaOS-2 cells were treated for 16 hours with increasing concentrations of Palm (0.125 mM to 0.50 mM) ± 0.25 mM Ole. A, Lipid droplets were identified by Oil Red staining. B, Total cellular neutral lipids content and FA composition were evaluated by gas chromatography. Values are expressed relative to Ctrl and are means of 3 individual experiments.

with their higher susceptibility to lipotoxicity. Moreover, we established that Ole exerts its protective action by abolishing Palm-induced ER dysfunctions. The ER plays a pivotal role in the regulation of lipid and protein metabolism. The accumulation of misfolded proteins or other stressors in the ER initiates a cellular adaptive program, known as the UPR, to re-establish the cellular equilibrium: while the inhibition of general protein synthesis prevents further overloading of the ER, the simultaneous production of specific chaperones favors the refolding of misfolded proteins. However, prolonged or extreme ER stress overwhelms the normal ER protein folding machinery, triggers activation of proapoptotic genes and leads to cell death (63).

In situations of excessive FA exposure, the relative toxicity of FA is related to their capacity to be directed to distinct metabolic fates. For example, palmitoylation was recently implicated in Palm-induced toxicity in human osteoblasts (36). On the other hand, it it is known that Palm is poorly incorporated into TG and causes apoptosis whereas Ole stimulates TG accumulation and is well tolerated. Monounsaturated FA thus promote the detoxification of saturated FA by fostering their esterification into TG so that the potentially toxic lipids are safely stored within LD (71). LD formation in nonadipose cells in response to lipid overload was therefore proposed as an initial cellular defense against lipotoxicity (72). The role of TG accumulation in cell survival is however somewhat controversial. In the insulin producing pancreatic beta cells, it was described as cytotoxic (73) or cytoprotective (37).

We thus evaluated the capacity of Palm and Ole to induce LD formation in osteoblastic cells. Ole, but not Palm, triggers LD formation and increases the cellular neutral lipids content. Moreover, in the concomitant presence of Palm, Ole favors the incorporation of the saturated FA into the neutral lipids fraction. These observations suggest that Ole promotes FA storage and may therefore serve its protective function by favoring Palm esterification and incorporation into stable LD.

In conclusion, several pathways are involved in Palm-induced toxicity in human MSC and osteoblastic cells. The lipotoxic action exerted on osteoblastic cells by Palm is prevented by the monounsaturated FA Ole via induction of TG synthesis and inhibition of ERK activation and ER stress initiation. In addition, Palm, but not Ole has a pro-inflammatory effect that may compromise bone health.

Interestingly, Drosatos-Tampakaki et al has recently shown that Palm is not toxic for osteoclasts, the bone resorbing cells and enhances osteoclastogenesis, thus favoring bone resorption (74). On the contrary, Ole does not support osteoclast differentiation but inhibits Palm-induced osteoclastogenesis by increasing TG accumulation and inducing LD formation (74).

The present study, combined with the work of Drosatos-Tampakaki et al, demonstrates that saturated and mono-unsaturated FA have opposite actions on osteoblasts and osteoclasts. Therefore, while Palm could impair bone formation and promote bone resorption, Ole could have a protective action on bone cells by counteracting those effects. Further studies should now be pursued in animal models of bone diseases associated with alterations of lipid metabolism, such as osteoporosis, to establish the impact of FA on bone mass and evaluate whether the manipulation of dietary fatty acid composition could affect skeletal health.

Acknowledgments

We thank Jessica Lechanteur for technical support and Dr Laurence Lagneaux for the gift of MSC isolated from Wharton jelly.

The present study was supported by the Fonds National de la Recherche Scientifique (convention J.088.13CDR) and by the Daiichi Sankyo-Belgian Bone Club Young Investigator Award.

Address all correspondence and requests for reprints to: Prof. Joanne Rasschaert, Ph.D., Laboratory of Bone and Metabolic Biochemistry, Faculty of Medicine, Université libre de Bruxelles, 808 Route de Lennik, 1070, Brussels, Belgium, Email: jrasscha@ulb.ac.be, Phone: +3225556307 Fax+3225556230.

Disclosure Summary: The authors have nothing to disclose.

This work was supported by .

References

1. **Brown SA, Rosen CJ.** *Osteoporosis. Med Clin North Am*. 2003; 87(5):1039–1063.
2. **Le Blanc K, Pittenger MF.** Mesenchymal stem cells: progress toward promise. *Cytotherapy*. 2005;7(1):36–45.
3. **Huang W, Yang S, Shao J, Li YP.** Signaling and transcriptional regulation in osteoblast commitment and differentiation. *Front Biosci*. 2007;12:3068–3092.
4. **Weinstein RS, Manolagas SC.** Apoptosis and Osteoporosis. *Am J Med*. 2000;108:153–164.
5. **Verma S, Rajaratnam JH, Denton J, Hoyland JA, Byers RJ.** Adipocytic proportion of bone marrow is inversely related to bone formation in osteoporosis. *J Clin Pathol*. 2002;55(9):693–698.
6. **Cohen A, Dempster DW, Stein EM, Nickolas TL, Zhou H, McMahon DJ, Müller R, Kohler T, Zwahlen A, Lappe JM, Young P, Recker R, Shane.** Increased marrow adiposity in premenopausal women with idiopathic osteoporosis. *J Clin Endocrinol Metab*. 2012;97(8):2782–2791.
7. **Bouillon R, Bex M, Van Herck E, Laureys J, Dooms L, Lesaffre E, Ravussin E.** Influence of age, sex, and insulin on osteoblast function: osteoblast dysfunction in diabetes mellitus. *J Clin Endocrinol Metab*. 1995;80(4):1194–1202.
8. **Georgiou KR, Hui SK, Xian CJ.** Regulatory pathways associated with bone loss and bone marrow adiposity caused by aging, che-

motherapy, glucocorticoid therapy and radiotherapy. *Am J Stem Cells*. 2012;1(3):205–224.
9. **Gimble JM, Robinson CE, Wu X, Kelly KA, Rodriguez BR, Kliewer SA, Lehmann JM, Morris DC.** Peroxisome proliferator-activated receptor-gamma activation by thiazolidinediones induces adipogenesis in bone marrow stromal cells. *Mol Pharmacol*. 1996;50(5): 1087–1094.
10. **Fazeli PK, Horowitz MC, MacDougald OA, Scheller EL, Rodeheffer MS, Rosen CJ, Klibanski A.** Marrow fat and bone: new perspectives. *J Clin Endocrinol Metab*. 2013;98(3):935–945.
11. **Ahima RS, Flier JS.** Adipose tissue as an endocrine organ. *Trends Endocrinol Metab*. 2000;11(8):327–332.
12. **Frühbeck G, Gómez-Ambrosi J, Muruzábal FJ, Burrell MA.** The adipocyte: a model for integration of endocrine and metabolic signaling in energy metabolism regulation. *Am J Physiol Endocrinol Metab*. 2001;280(6):E827–847.
13. **Lecka-Czernik B.** Marrow fat metabolism is linked to the systemic energy metabolism. *Bone*. 2012;50(2):534–539.
14. **Rosen CJ, Bouxsein ML.** Mechanisms of disease: is osteoporosis the obesity of bone? *Nat Clin Pract Rheumatol*. 2006;2(1):35–43.
15. **Rosen CJ, Ackert-Bicknell C, Rodriguez JP, Pino AM.** Marrow fat and the bone microenvironment: developmental, functional, and pathological implications. *Crit Rev Eukaryot Gene Expr*. 2009; 19(2):109–124.
16. **Kawai M, de Paula FJA, Rosen CJ.** New Insights into Osteoporosis : The Bone-Fat Connection. *J Intern Med*. 2012;272(4):317–329.
17. **Unger RH.** Lipotoxic Diseases. *Annu Rev Med*. 2002;53(1):319–336.
18. **Turpin SM, Lancaster GI, Darby I, Febbraio MA, Watt MJ.** Apoptosis in skeletal muscle myotubes is induced by ceramides and is positively related to insulin resistance. *Am J Physiol Endocrinol Metab*. 2006;291(6):E1341–1350.
19. **Malhi H, Bronk SF, Werneburg NW, Gores GJ.** Free fatty acids induce JNK-dependent hepatocyte lipoapoptosis. *J Biol Chem*. 2006;281(17):12093–12101.
20. **Unger RH, Zhou YT.** Lipotoxicity of beta-cells in obesity and in other causes of fatty acid spillover. *Diabetes*. 2001;50 Suppl 1:S118–121.
21. **Weinberg JM.** *Lipotoxicity. Kidney Int*. 2006;70(9):1560–1566.
22. **Maurin AC, Chavassieux PM, Frappart L, Delmas PD, Serre CM, Meunier PJ.** Influence of mature adipocytes on osteoblast proliferation in human primary cocultures. *Bone*. 2000;26(5):485–489.
23. **Clabaut A, Delplace S, Chauveau C, Hardouin P, Broux O.** Human osteoblasts derived from mesenchymal stem cells express adipogenic markers upon coculture with bone marrow adipocytes. *Differentiation*. 2010;80(1):40–45.
24. **Elbaz A, Wu X, Rivas D, Gimble JM, Duque G.** Inhibition of fatty acid biosynthesis prevents adipocyte lipotoxicity on human osteoblasts in vitro. *J Cell Mol Med*. 2010;14(4):982–991.
25. **Wang D, Haile A, Jones LC.** Dexamethasone-induced lipolysis increases the adverse effect of adipocytes on osteoblasts using cells derived from human mesenchymal stem cells. *Bone*. 2013;53(2): 520–530.
26. **Yeung DKW, Griffith JF, Antonio GE, Lee FK, Woo J, Leung PC.** Osteoporosis is associated with increased marrow fat content and decreased marrow fat unsaturation: a proton MR spectroscopy study. *J Magn Reson Imaging*. 2005;22(2):279–285.
27. **Patsch JM, Li X, Baum T, Yap SP, Karampinos DC, Schwartz AV, Link TM.** Bone marrow fat composition as a novel imaging biomarker in postmenopausal women with prevalent fragility fractures. *J Bone Miner Res*. 2013;28(8):1721–1728.
28. **Corwin RL, Hartman TJ, Maczuga SA, Graubard BI.** Nutritional epidemiology dietary saturated fat intake is inversely associated with bone density in humans: Analysis of NHANES III. *J Nutr*. 2006;136:159–165.
29. **Orchard TS, Cauley JA, Frank GC, Neuhouser ML, Robinson JG, Snetselaar L, Tylavsky F, Wactawski-Wende J, Young AM, Lu B, Jackson RD.** Fatty acid consumption and risk of fracture in the Women's Health Initiative. *Am J Clin Nutr*. 2010;92(6):1452–1460.
30. **Baylin A, Kabagambe EK, Siles X, Campos H.** Adipose tissue biomarkers of fatty acid intake. *Am J Clin Nutr*. 2002;76(4):750–757.
31. **Kim J, Ahn M, Baek S, Lee IK, Kim Y-W, Kim J-Y, Dan J-M, Park S-Y.** AMPK activator, AICAR, inhibits palmitate-induced apoptosis in osteoblast. Bone. 2008;43:394–404.
32. **Eitel K, Staiger H, Brendel MD, Brandhorst D, Bretzel RG, Häring HU, Kellerer M.** Different role of saturated and unsaturated fatty acids in beta-cell apoptosis. *Biochem Biophys Res Commun*. 2002; 299(5):853–856.
33. **Jové M, Planavila A, Sánchez RM, Merlos M, Laguna JC, Vázquez-Carrera M.** Palmitate induces tumor necrosis factor-alpha expression in C2C12 skeletal muscle cells by a mechanism involving protein kinase C and nuclear factor-kappaB activation. *Endocrinology*. 2006;147(1):552–561.
34. **Dominici M, Le Blanc K, Mueller I, Slaper-Cortenbach I, Marini F, Krause D, Deans R, Keating A, Prockop DJ, Horwitz E.** Minimal criteria for defining multipotent mesenchymal stromal cells. *Cytotherapy*. 2006;8(4):315–317.
35. **Dong X, Bi L, He S, Meng G, Wei B, Jia S, Liu J.** FFAs-ROS-ERK/P38 pathway plays a key role in adipocyte lipotoxicity on osteoblasts in co-culture. *Biochimie*. 2014;101:123–131.
36. **Gunaratnam K, Vidal C, Gimble JM, Duque G.** Mechanisms of palmitate-induced lipotoxicity in human osteoblasts. *Endocrinology*. 2014;155(1):108–116.
37. **Cnop M, Hannaert JC, Hoorens A, Eizirik DL, Pipeleers DG.** Inverse relationship between cytotoxicity of free fatty acids in pancreatic islet cells and cellular triglyceride accumulation. *Diabetes*. 2001; 50(8):1771–1777.
38. **Larionov A, Krause A, Miller W.** A standard curve based method for relative real time PCR data processing. *BMC Bioinformatics*. 2005; 6(62):1–16.
39. **Louis C, Van den Daelen C, Tinant G, Bourez S, Thomé JP, Donnay I, Larondelle Y, Debier C.** Efficient in vitro adipocyte model of long-term lipolysis: a tool to study the behavior of lipophilic compounds. *In Vitro Cell Dev Biol Anim*. 2014;50(6):507–518.
40. **Chang J, Wang Z, Tang E, Fan Z, McCauley L, Franceschi R, Guan K, Krebsbach PH, Wang CY.** Inhibition of osteoblastic bone formation by nuclear factor-kappaB. *Nat Med*. 2009;15(6):682–689.
41. **Potier E, Ferreira E, Andriamanalijaona R, Pujol JP, Oudina K, Logeart-Avramoglou D, Petite H.** Hypoxia affects mesenchymal stromal cell osteogenic differentiation and angiogenic factor expression. *Bone*. 2007;40(4):1078–1087.
42. **Ryu JM, Lee MY, Yun SP, Han HJ.** High glucose regulates cyclin D1/E of human mesenchymal stem cells through TGF-beta1 expression via Ca2+/PKC/MAPKs and PI3K/Akt/mTOR signal pathways. *J Cell Physiol*. 2010;224(1):59–70.
43. **Huang S, Rutkowsky JM, Snodgrass RG, Ono-Moore KD, Schneider DA, Newman JW, Adams SH, Hwang DH.** Saturated fatty acids activate TLR-mediated proinflammatory signaling pathways. *J Lipid Res*. 2012;53(9):2002–2013.
44. **Raicevic G, Najar M, Stamatopoulos B, De Bruyn C, Meuleman N, Bron D, Toungouz M, Lagneaux L.** The source of human mesenchymal stromal cells influences their TLR profile as well as their functional properties. *Cell Immunol*. 2011;270(2):207–216.
45. **Lu J, Wang Q, Huang L, Dong H, Lin L, Lin N, Zheng F, Tan J.** Palmitate causes endoplasmic reticulum stress and apoptosis in human mesenchymal stem cells: prevention by AMPK activator. *Endocrinology*. 2012;153(11):5275–5284.
46. **Greenberg AS, Coleman RA.** Expanding roles for lipid droplets. *Trends Endocrinol Metab*. 2011;22(6):195–196.
47. **Justesen J, Stenderup K, Ebbesen EN, Mosekilde L, Steiniche T, Kassem M.** Adipocyte tissue volume in bone marrow is increased with aging and in patients with osteoporosis. *Biogerontology*. 2001; 2(3):165–171.

48. **Hardouin P, Pansini V, Cortet B.** Bone marrow fat. *Joint Bone Spine*. 2014;81(4):313–319.
49. **Doucette CR, Horowitz MC, Berry R, MacDougald OA, Anunciado-Koza R, Koza RA, Rosen CJ.** A high fat diet increases bone marrow adipose tissue (MAT) but does not alter trabecular or cortical bone mass in C57BL/6J mice. *J Cell Physiol*. 2015;230(9): 2032–2037.
50. **Chen JR, Lazarenko OP, Wu X, Tong Y, Blackburn ML, Shankar K, Badger TM, Ronis MJJ.** Obesity reduces bone density associated with activation of PPARγ and suppression of Wnt/β-catenin in rapidly growing male rats. *PLoS One*. 2010;5(10):1–13.
51. **Patsch JM, Kiefer FW, Varga P, Pail P, Rauner M, Stupphann D, Resch H, Moser D, Zysset PK, Stulnig TM, Pietschmann P.** Increased bone resorption and impaired bone microarchitecture in short-term and extended high-fat diet-induced obesity. *Metabolism*. 2011;60(2):243–249.
52. **Lecka-Czernik B, Stechschulte LA, Czernik PJ, Dowling AR.** High bone mass in adult mice with diet-induced obesity results from a combination of initial increase in bone mass followed by attenuation in bone formation; implications for high bone mass and decreased bone quality in obesity. *Mol Cell Endocrinol*. 2015;15:410:35–41.
53. **Reid IR.** *Fat and bone. Arch Biochem Biophys*. 2010;503(1):20–27.
54. **Villareal DT, Apovian CM, Kushner RF, Klein S.** Obesity in older adults : technical review and position statement of the American Society for Nutrition and NAASO, The Obesity Society. *Am J Clin Nutr*. 2005;82:923–934.
55. **Compston JE, Watts NB, Chapurlat R, Cooper C, Boonen S, Greenspan S, Pfeilschifter J, Silverman S, Díez-Pérez A, Lindsay R, Saag KG, Netelenbos JC, Gehlbach S, Hooven FH, Flahive J, Adachi JD, Rossini M, Lacroix AZ, Roux C, Sambrook PN, Siris ES.** Glow Investigators. Obesity is not protective against fracture in postmenopausal women: GLOW. *Am J Med*. 2011;124(11):1043–1050.
56. **Zhang P, Peterson M, Su GL, Wang SC.** Visceral adiposity is negatively associated with bone density and muscle attenuation. *Am J Clin Nutr*. 2015;101(2):337–343.
57. **Wren TAL, Chung SA, Dorey FJ, Bluml S, Adams GB, Gilsanz V.** Bone marrow fat is inversely related to cortical bone in young and old subjects. *J Clin Endocrinol Metab*. 2011;96(3):782–786.
58. **Shen W, Chen J, Gantz M, Punyanitya M, Heymsfield SB, Gallagher D, Albu J, Engelson E, Kotler D, Pi-Sunyer X, Gilsanz V.** MRI-measured pelvic bone marrow adipose tissue is inversely related to DXA-measured bone mineral in younger and older adults. *Eur J Clin Nutr*. 2012;66(9):983–988.
59. **Devlin MJ.** Bone marrow composition, diabetes, and fracture risk: more bad news for saturated fat. *J Bone Miner Res*. 2013;28(8): 1718–1720.
60. **Schwartz AV.** Marrow fat and bone: review of clinical findings. *Front Endocrinol*. 2015;6(40):1–6.
61. **Fillmore N, Huqi A, Jaswal JS, Mori J, Paulin R, Haromy A, Onay-Besikci A, Ionescu L, Thébaud B, Michelakis E, Lopaschuk GD.** Effect of fatty acids on human bone marrow mesenchymal stem cell energy metabolism and survival. *PLoS One*. 2015;10(3):1–17.
62. **Smith AN, Muffley LA, Bell AN, Numhom S, Hocking AM.** Unsaturated fatty acids induce mesenchymal stem cells to increase secretion of angiogenic mediators. *J Cell Physiol*. 2012;227(9):3225–3233.
63. **Hotamisligil GS.** Endoplasmic reticulum stress and the inflammatory basis of metabolic disease. *Cell*. 2010;140(6):900–917.
64. **Mundy GR.** *Osteoporosis and Inflammation*. 2007;65(12):S147–S151.
65. **Dasu MR, Ramirez S, Isseroff RR.** Toll-like receptors and diabetes: a therapeutic perspective. *Clin Sci (Lond)*. 2012;122(5):203–214.
66. **Tamura T, Udagawa N, Takahashi N, Miyaura C, Tanaka S, Yamada Y, Koishihara Y, Ohsugi Y, Kumaki K, Taga T.** Soluble interleukin-6 receptor triggers osteoclast formation by interleukin 6. *Proc Natl Acad Sci U S A*. 1993;90(24):11924–11928.
67. **Bendre MS, Montague DC, Peery T, Akel NS, Gaddy D, Suva LJ.** Interleukin-8 stimulation of osteoclastogenesis and bone resorption is a mechanism for the increased osteolysis of metastatic bone disease. *Bone*. 2003;33(1):28–37.
68. **Houssiau FA, Devogelaer JP, Van Damme J, de Deuxchaisnes CN, Van Snick J.** Interleukin-6 in synovial fluid and serum of patients with rheumatoid arthritis and other inflammatory arthritides. *Arthritis Rheum*. 1988;31(6):784–788.
69. **Lisignoli G, Toneguzzi S, Pozzi C, Piacentini A, Riccio M, Ferruzzi A, Gualtieri G, Facchini A.** Proinflammatory cytokines and chemokine production and expression by human osteoblasts isolated from patients with rheumatoid arthritis and osteoarthritis. *J Rheumatol*. 1999;26(4):791–799.
70. **Karaskov E, Scott C, Zhang L, Teodoro T, Ravazzola M, Volchuk A.** Endoplasmic reticulum stress, which may contribute to INS-1 pancreatic β-cell apoptosis. 2006;147(7):3398–3407.
71. **Listenberger LL, Han X, Lewis SE, Cases S, Farese RV Jr., Ory DS, Schaffer JE.** Triglyceride accumulation protects against fatty acid-induced lipotoxicity. *Proc Natl Acad Sci U S A*. 2003;100(6):3077–3082.
72. **Peng G, Li L, Liu Y, Pu J, Zhang S, Yu J, Zhao J, Liu P.** Oleate blocks palmitate-induced abnormal lipid distribution, endoplasmic reticulum expansion and stress, and insulin resistance in skeletal muscle. *Endocrinology*. 2011;152(6):2206–2218.
73. **Briaud I, Harmon JS, Kelpe CL, Segu VB, Poitout V.** Lipotoxicity of the pancreatic beta-cell is associated with glucose-dependent esterification of fatty acids into neutral lipids. *Diabetes*. 2001;50(2):315–321.
74. **Drosatos-Tampakaki Z, Drosatos K, Siegelin Y, Gong S, Khan S, Van Dyke T, Goldberg IJ, Schulze PC, Schulze-Späte U.** Palmitic acid and DGAT1 deficiency enhance osteoclastogenesis, while oleic acid-induced triglyceride formation prevents it. *J Bone Miner Res*. 2014;29(5):1183–1195.